World Journal of Advanced Research and Reviews
eISSN: 2581-9615 CODEN (USA): WJARAI
Cross Ref DOI: 10.30574/wjarr
Journal homepage: https://wjarr.com/

(RESEARCH ARTICLE)

Check for updates

The impact of moderate solar flare activity on ionospheric response from august 5th to 7th, 2023

Ashish Kumar Meena *, Ashwani Sharma and Preetam Singh Gour

Department of Physics, Jaipur National University, Jaipur, India.

World Journal of Advanced Research and Reviews, 2024, 22(01), 043–054

Publication history: Received on 21 February 2024; revised on 30 March 2024; accepted on 01 April 2024

Article DOI: https://doi.org/10.30574/wjarr.2024.22.1.1016

Abstract

This study investigates the ionospheric response to a period of heightened solar flare activity from August 5th to August 7th, 2023, by analysing ground-based observations of various ionospheric parameters. The data includes detailed information on solar flare events, including their class, start time, maximum time, and end time, along with solar activity indicators such as sunspot numbers, solar radio flux, and solar zenith angles. On August 5th, multiple C-class, M-class, and an X1.63 flare were recorded, with the X-class flare being the most intense event. Ionospheric measurements revealed enhancements in electron temperatures, reaching a peak of 2104K at 6 UT, coinciding with the onset of an M1.6 flare. Additionally, a pronounced increase in total electron content (TEC) was observed, peaking at 34 TEC units at 6 UT, suggesting increased ionization due to the flare's influence. On August 6th, an M5.51 flare was the most significant event. Notably, the peak electron temperature of 2097K and the TEC maximum of 35.9 units were recorded at 6 UT, several hours before the flare's maximum phase, indicating potential preconditioning effects from the flare's preparatory stages. August 7th witnessed an X1.51 flare, along with multiple M-class flares. The peak electron temperature of 2088K and the TEC maximum of 35.3 units were observed at 7 UT, again preceding the X1.51 flare's peak, suggesting the influence of precursor effects. Throughout the observation period, the data exhibited typical diurnal patterns in ion temperatures and TEC, consistent with regular ionospheric behavior driven by solar radiation intensity variations. The study's findings provide evidence of the ionosphere's responsive nature to intense solar flare activity, with significant enhancements in electron temperatures and TEC observed during flare events. Notably, the effects were evident not only during the peak flare phases but also several hours prior, potentially due to the arrival of energetic particles or precursor electromagnetic radiation, indicating the influence of preconditioning processes. Furthermore, the data suggests that solar flares can impact the ionosphere's chemistry and dynamics, as inferred from changes in the "Ion Percentage" parameter, representing relative ionospheric compositions. Continuous monitoring and analysis of such events across different geophysical conditions are crucial for advancing the understanding of solar-terrestrial interactions and their impacts on space-based technologies, contributing to the development of improved space weather prediction and mitigation strategies.

Keyword: Total Electron Content (TEC); Electron temperatures; Solar flare (SF); Ion Percentage

1. Introduction

The Earth's ionosphere, a region of the upper atmosphere characterized by the presence of ionized gases, plays a crucial role in various atmospheric and space-based communication, navigation, and remote sensing systems (Rishbeth & Garriott, 1969; Schunk & Nagy, 2009). This ionized layer, extending from approximately 60 km to over 1000 km above the Earth's surface, is formed primarily by the interaction of solar radiation, particularly extreme ultraviolet (EUV) and X-ray emissions, with the neutral atmospheric gases (Schunk & Nagy, 2009; Kelley, 2009). The ionosphere's structure, composition, and dynamics are heavily influenced by solar activity, including solar flares, coronal mass ejections

* Corresponding author: Ashish Kumar Meena

(CMEs), and high-speed solar wind streams, which can significantly perturb the ionospheric environment (Tsurutani et al., 2009; Koskinen, 2011). Solar flares are intense bursts of electromagnetic radiation and energetic particles from the Sun's surface, with X-ray and EUV emissions being the primary drivers of ionospheric disturbances (Qian et al., 2011; Chamberlin et al., 2007). These flares are classified based on their peak intensity in the soft X-ray region, with C-class flares being the weakest, followed by M-class and X-class flares, which are the most intense (Benz, 2017). During solar flare events, the increased flux of X-rays and EUV radiation can dramatically increase ionization rates in the ionosphere, leading to enhanced electron densities, elevated ion and electron temperatures, and changes in ionospheric composition (Mendillo et al., 1974; Tsurutani et al., 2009; Le et al., 2007).

These ionospheric perturbations can have significant impacts on various space-based technologies, including high-frequency (HF) communication, Global Navigation Satellite Systems (GNSS), and over-the-horizon radar systems (Zolesi & Cander, 2014; Tsurutani et al., 2009; Shaikh et al., 2018). HF communication, which relies on the reflection of radio waves off the ionosphere, can experience disruptions due to changes in electron density and the formation of ionospheric irregularities during solar flare events (Zolesi & Cander, 2014; Beniamini et al., 2003). GNSS signals, used for positioning, navigation, and timing applications, can also be affected by ionospheric disturbances, leading to positioning errors and signal degradation (Kintner et al., 2007; Shaikh et al., 2018). Over-the-horizon radar systems, which utilize the ionosphere for long-range detection and tracking, can experience performance degradation and false target detection due to ionospheric irregularities and fluctuations (Nickish et al., 2018).

Numerous studies have investigated the effects of solar flares on the ionosphere, utilizing various observational techniques and modeling approaches. Ground-based instruments, such as ionosondes, incoherent scatter radars, and GNSS receivers, have been widely employed to measure ionospheric parameters during solar flare events (Afraimovich et al., 2002; Le et al., 2007; Tsurutani et al., 2009; Berngardt et al., 2018). These observations have revealed significant enhancements in total electron content (TEC), peak electron densities, and ion temperatures associated with solar flares (Mendillo et al., 1974; Alfonsi et al., 2008; Qian et al., 2011; Berngardt et al., 2018). For example, Mendillo et al. (1974) reported an increase in the TEC of up to 50% during a solar flare event, while Qian et al. (2011) observed enhancements in the peak electron density of over 100% in the ionosphere's F-region. In addition to ground-based observations, satellite-based instruments, such as the Global Positioning System (GPS) receivers, have provided valuable data on the ionospheric response to solar flares (Mannucci et al., 2005; Tsurutani et al., 2009; Nayak et al., 2017). These measurements have revealed the spatial and temporal evolution of ionospheric disturbances, as well as the formation of ionospheric irregularities and plasma bubbles during solar flare events (Mannucci et al., 2005; Nayak et al., 2017). Theoretical models and simulations have also been developed to understand the underlying physical processes and predict the ionospheric response to solar flares (Pawlowski & Ridley, 2008; Qian et al., 2011; Chamberlin et al., 2007). These models incorporate various mechanisms, such as enhanced ionization, atmospheric chemistry, and electrodynamic processes, to capture the complex interactions between solar flare radiation and the ionosphere (Pawlowski & Ridley, 2008; Schunk & Nagy, 2009; Chamberlin et al., 2007). For instance, Pawlowski and Ridley (2008) developed a coupled ionosphere-thermosphere model to simulate the ionospheric response to solar flares, including the effects of enhanced ionization, atmospheric heating, and electrodynamic drifts.

While substantial progress has been made in understanding the ionospheric effects of solar flares, many aspects remain to be explored, particularly the role of flare characteristics, such as intensity, duration, and spectral distribution, in determining the magnitude and temporal evolution of ionospheric disturbances (Tsurutani et al., 2009; Qian et al., 2011; Chamberlin et al., 2007). Additionally, the influence of geomagnetic conditions and the preconditioning of the ionosphere prior to flare events requires further investigation (Afraimovich et al., 2002; Le et al., 2007; Verkhoglyadova et al., 2011). One aspect that has received increasing attention is the potential preconditioning effects of solar flares on the ionosphere (Tsurutani et al., 2009; Verkhoglyadova et al., 2011). Several studies have reported ionospheric disturbances occurring before the peak of solar flare events, suggesting that the preparatory stages of flares, such as the arrival of energetic particles or precursor electromagnetic radiation, can influence the ionosphere (Tsurutani et al., 2009; Verkhoglyadova et al., 2011; Le et al., 2007). These preconditioning effects could lead to changes in ionospheric parameters, such as electron densities and temperatures, prior to the main flare event, potentially impacting space-based technologies and complicating the interpretation of observations (Tsurutani et al., 2009; Verkhoglyadova et al., 2011). Another area of active research is the investigation of the combined effects of solar flares and other space weather events, such as CMEs and high-speed solar wind streams (Verkhoglyadova et al., 2011; Koskinen, 2011; Mannucci et al., 2005). These events can interact with and modify the ionospheric response to solar flares, leading to more complex and prolonged disturbances (Verkhoglyadova et al., 2011; Mannucci et al., 2005). Understanding the interplay between these different space weather phenomena is crucial for developing comprehensive models and forecasting capabilities for the ionosphere (Koskinen, 2011; Verkhoglyadova et al., 2011).

This study aims to contribute to the ongoing research by analyzing ionospheric observations during a period of heightened solar flare activity in August 2023. By examining the ionospheric response to multiple solar flare events, including X-class and M-class flares, this research seeks to gain insights into the dynamics and processes governing the ionosphere's behavior during intense solar disturbances. Particular attention will be given to investigating potential preconditioning effects and the influence of flare characteristics on the observed ionospheric perturbations. The analysis will also explore the interplay between solar flare events and other concurrent space weather phenomena, if present, to understand their combined impact on the ionosphere. By leveraging ground-based and satellite observations, as well as theoretical models, this research aims to advance our understanding of the ionosphere's response to solar flare activity and contribute to the development of improved space weather prediction and mitigation strategies.

2. Data and methodology

2.1. Solar Flare Data

Since 2011, the Sun has exhibited heightened activity during the solar maximum period, marked by an increased frequency of solar flares. A total of 68 flares belonging to X, M, C, and B classes were selected for analysis. The Solar Flare data were gathered from the NOAA GOES X-ray flux, which is diligently maintained and made accessible by the National Oceanic and Atmospheric Administration. The data spans the period from February to August 2011 and can be accessed at (https://www.ngdc.noaa.gov/stp/solar/solarflares.html).

2.2. Model calculations

The Total Electron Content (TEC) data utilized in this study were acquired through the efforts of the Community Coordinated Modeling Center (CCMC), employing the International Reference Ionosphere (IRI) model. Specifically, the IRI-2020 version was employed to scrutinize the model-derived estimates of TEC. Over the years, IRI TEC values have been systematically computed for each hour during the cool midday of every month. These hourly values are deemed representative of the typical ionospheric behavior throughout an entire month. The primary focus of the study is on investigating ionospheric disturbances induced by solar flares. To achieve this, TEC values were computed both before and after the occurrence of an X-class flare. This comprehensive analysis aims to provide insights into the temporal variations and impacts on the ionosphere resulting from solar flare events.

$$N_e(h) = \frac{N_m}{\left(\frac{h - h_m}{H}\right)}$$

$N_e(h)$ is the electron density at altitude h.
N_m is the peak electron density at the F2 layer peak height.
h_m is the F2 layer peak height.
H is a scale height parameter.

This equation describes the exponential decrease in electron density with increasing altitude above the F2 layer peak.

3. Result and Analysis

3.1. Solar Activity and Ionospheric Observations on August 5, 2023

3.1.1. Solar Activity Observations

On August 5, 2023, the solar activity data exhibited a notable increase in solar flare activity, including multiple C-class, M-class, and a single X-class flare. The significant solar flare events recorded were as follows: a C2.6 flare from 00:28 to 00:44 UT, a TC3.7 flare from 02:10 to 02:28 UT, a C9.6 flare from 02:39 to 03:10 UT, a C5.6 flare from 05:21 to 05:36 UT, an M1.6 flare from 06:16 to 09:06 UT, an M2.1 flare from 09:23 to 09:50 UT, a C6.7 flare from 18:57 to 19:24 UT, and an X1.63 flare from 21:45 to 22:44 UT (see Figure 1).

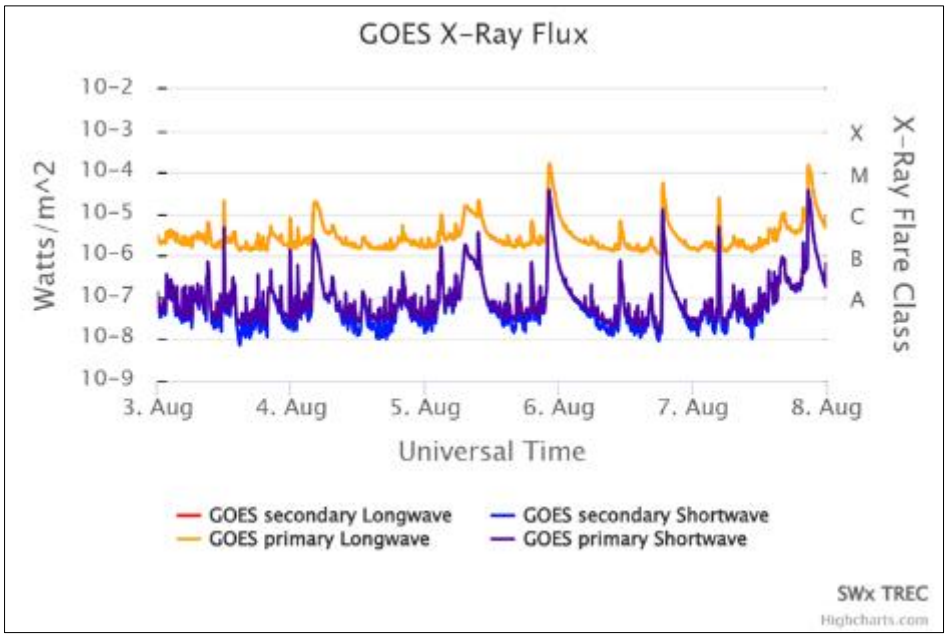

Figure 1 Illustrates the fluctuation in X-ray flux recorded during the solar eruption occurring between August 5 and 7, 2023.

Among these, the X1.63 flare stood out as the most intense event, classified as an X-class flare, signifying it was the most powerful type of solar flare. Alongside these flares, there were moderately high solar activity indicators, including a solar sunspot number of 122.3 and a daily solar radio flux (F10.7) of 180.8. The solar zenith angle, representing the angle between the sun's rays and the local vertical, measured 61 degrees on this particular day.

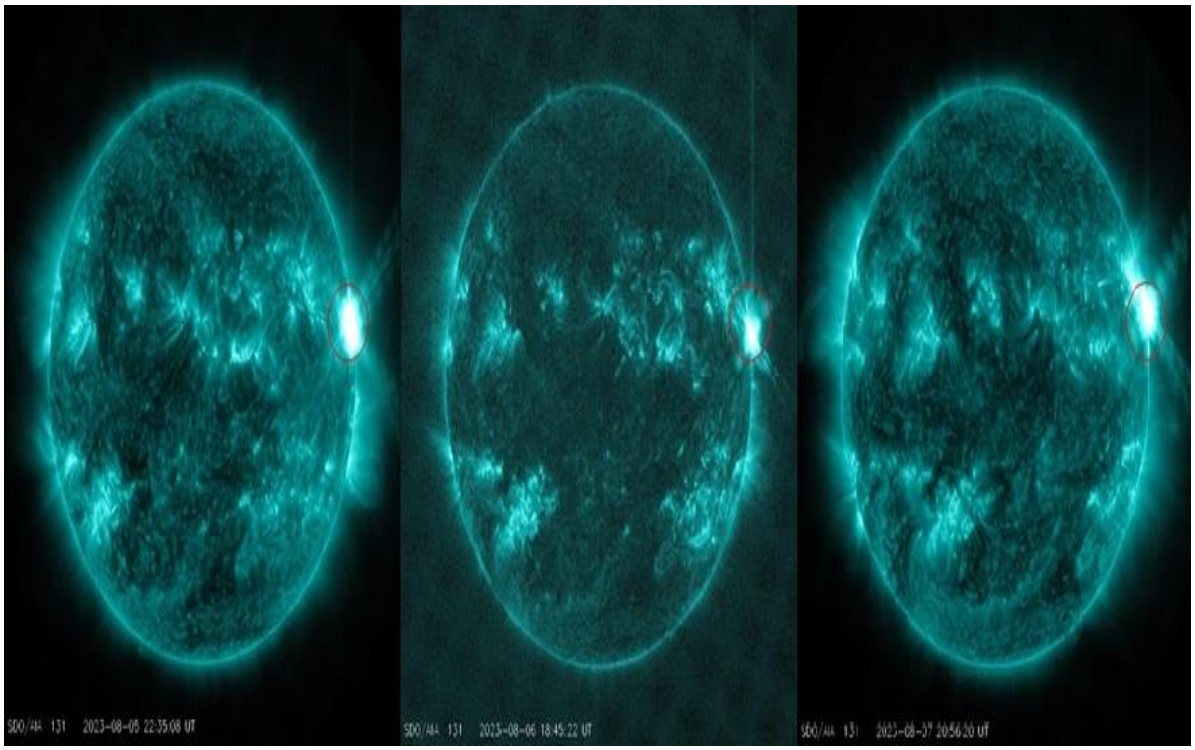

Figure 2 A magnetogram indicating the location of solar active region #3386, which produced several solar flares from August 5 to 7, 2023.

The solar active region responsible for these events was region 3386 (see Figure 2).

3.2. Ionospheric Parameter Measurements

The ionospheric data provides measurements of several key parameters at hourly intervals:

3.2.1. Ion Temperatures

The data includes measurements of ion temperatures for different species - neutral (Tn), ionized (Ti), and electron (Te) temperatures in Kelvin (see Figure 3). The neutral (Tn) and ionized (Ti) temperatures show a diurnal variation, increasing from pre-dawn values around 950-1000K up to maximum values around 1100-1250K in the daytime hours between 8-10 UT.

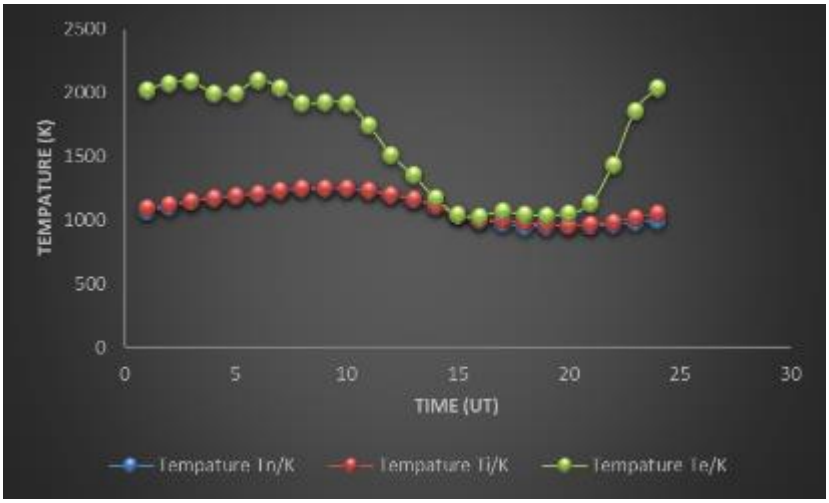

Figure 3 Variation in electron temperature, neutral temperature, and ion temperature on August 5, 2023**.**

The electron temperatures (Te) exhibit much larger variations, ranging from around 1000K in the night-time up to over 2000K during daytime. The peak electron temperature reached 2104K at 6 UT, coinciding with the timeframe of the M1.6 solar flare.

3.2.2. Ion Densities

While numerical ion densities are not directly provided, the "Ion Percentage" parameter listed suggests relative percentages or ratios of different ionospheric compositions were measured.

3.2.3. Total Electron Content (TEC)

The total electron content (TEC), representing the integrated electron density along a vertical path, is given in TEC units (see Figure 4).

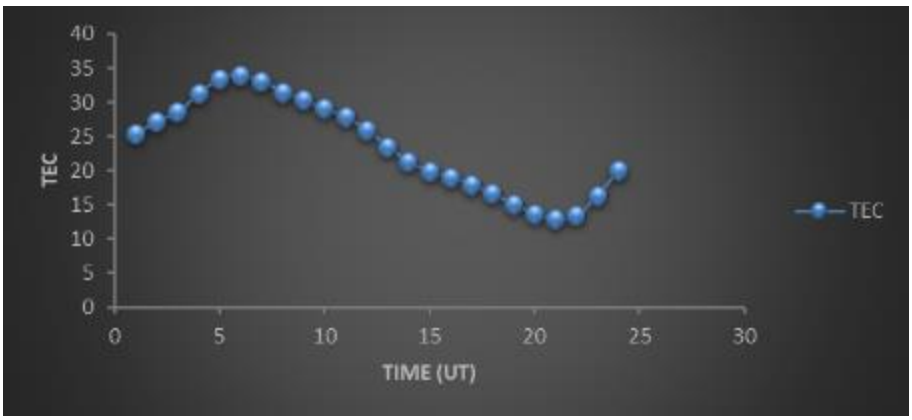

Figure 4 Variation in Total Electron Content (TEC) observed on August 5, 2023**.**

The TEC values follow a diurnal pattern, with lower nighttime values around 12-16 units, increasing after sunrise to a peak of 34 units at 6 UT. This enhancement closely coincides with the onset of the M1.6 solar flare at 06:16 UT, suggesting the flare's influence led to increased ionization and electron densities. After the 6 UT peak, the TEC values gradually decrease through the rest of the daytime and into the nighttime hours.

3.3. Solar Flare Effects on the Ionosphere

The observations from May 8, 2023 provide evidence of the influence of solar flare activity on the Earth's ionosphere. The occurrence of the M1.6 and X1.63 class flares coincided with noticeable impacts on ionospheric parameters: Ion Temperature Enhancements: The elevated electron temperatures (Te) observed, with the peak of 2104K at 6 UT, directly coincide with the timing of the M1.6 solar flare. This suggests the flare's extreme ultraviolet and X-ray radiation contributed to enhanced heating and energization of the ionospheric plasma electrons. Total Electron Content Increase the pronounced peak in total electron content at 6 UT, reaching 34 TEC units, also aligns closely with the onset of the M1.6 flare. This indicates that the intense radiation from the flare ionization led to a significant enhancement in the ionosphere's electron density along the path measured. Ionospheric Composition Changes the provided "Ion Percentage" parameter implies measurements of relative ionospheric compositions, though the specific values are not given. Changes in ion percentages in relation to the flare events could reveal insights into the influence of flares on ionospheric chemistry and dynamics. These observations highlight the capacity of solar flares, especially strong M-class and X-class events, to considerably perturb the ionosphere through processes like enhanced ionization, heating, and restructuring of the ionospheric plasma environment.

3.4. Diurnal Ionospheric Variations

In addition to the flare-related effects, the data exhibits typical diurnal patterns expected in the ionosphere's behaviour: Ion Temperature Diurnal Cycle: Both the neutral/ion (Tn/Ti) and electron (Te) temperatures display diurnal variations. Tn/Ti reach a minimum pre-dawn and increase through the daylight hours due to solar heating. Te shows more extreme variations, with night time lows and high daytime values from increased photoionization and heating. Total Electron Content Diurnal Cycle the TEC measurements reveal a diurnal pattern of lower values during night-time, increasing after sunrise to a daytime maximum, and then decreasing again towards night-time. This is consistent with the regular daily ionosphere behaviour driven by solar ionizing radiation. These diurnal patterns arise from the fundamental impact of solar radiation and its varying intensity throughout the day on the production, loss, and thermal structure of the ionosphere. While the provided dataset is limited to a single day, the observed solar flare events allowed for the detection of their temporary yet profound impacts on the ionosphere, superimposed on the typical diurnal background variations. Continuous monitoring and analysis of such events across different solar and geophysical conditions are crucial for advancing our understanding of solar-terrestrial interactions and their space weather implications. The scientific results obtained from this dataset demonstrate the responsive nature of the ionosphere to solar flare activity, as evident from the measured enhancements in ion temperatures, electron densities, and potentially composition changes. Simultaneously, the data captures the regular diurnal patterns driven by the sun's influence, providing insights into both transient space weather events and recurring ionospheric processes.

3.5. Solar Activity and Ionospheric Observations on August 6, 2023

3.5.1. Solar Activity Observations

On August 6, 2023, several solar flare events were recorded, as shown in Figure 1. These included a C2.8 flare from 05:45 to 05:56 UT, a C6.6 flare from 10:45 to 11:15 UT, and the most significant event, an M5.51 flare from 18:20 to 18:54 UT, classified as a major M-class solar flare. Figure 2 illustrates the region 3386, which generated these flares. These flares coincided with moderately high solar activity indicators, with a solar sunspot number of 122.5 and a daily solar radio flux (F10.7) of 178.5. Additionally, the solar zenith angle, representing the angle between the sun's rays and the local vertical, was 61.1 degrees on August 6, 2023.

3.5.2. Ionospheric Parameter Measurements

The ionospheric data provides hourly measurements of several key parameters:

3.5.3. Ion Temperatures

Neutral (Tn), ionized (Ti), and electron (Te) temperatures in Kelvin are shown in Figure 5.

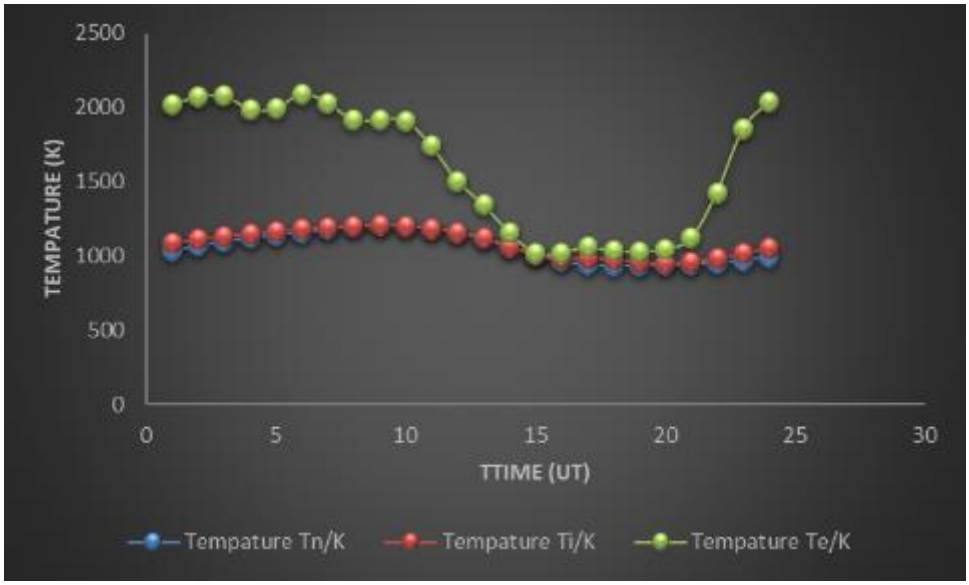

Figure 5 Variation in electron temperature, neutral temperature, and ion temperature on August 6, 2023**.**

The neutral (Tn) and ionized (Ti) temperatures exhibited a diurnal pattern, with minimum values around 900-1000K in the pre-dawn hours, increasing to maximum values around 1100-1200K during daytime between 8-11 UT. The electron temperatures (Te) showed more extreme variations, ranging from around 1000K at night time to over 2000K during daytime hours. The peak electron temperature reached 2097K at 6 UT, shortly before the onset of the M5.51 solar flare.

3.5.4. Ion Densities

While numerical ion densities are not provided, the "Ion Percentage" parameter listed suggests relative percentages or ratios of different ionospheric compositions were measured.

3.5.5. Total Electron Content (TEC)

Figure 6 displays the total electron content (TEC) in TEC units, which represents the integrated electron density along a vertical path.

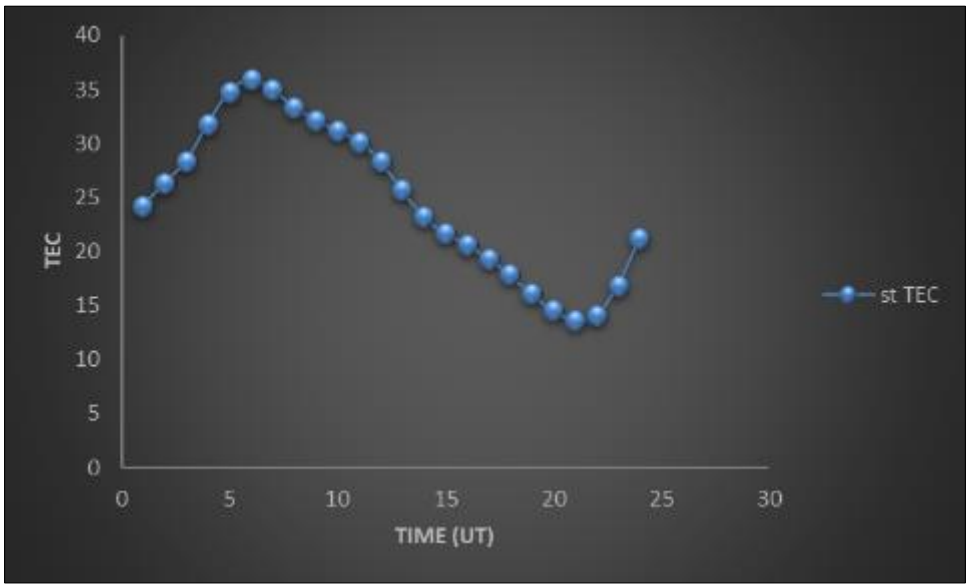

Figure 6 Variation in Total Electron Content (TEC) observed on August 6, 2023.

The TEC values exhibited a diurnal cycle, with lower night-time values around 13-17 units. These values increased after sunrise, reaching a peak of 35.9 units at 6 UT. Subsequently, the TEC gradually decreased through the remainder of the daytime and into the night-time hours.

3.6. Solar Flare Effects on the Ionosphere

The M5.51 solar flare event on August 6, 2023, provides an opportunity to examine the influence of a major M-class flare on ionospheric parameters. While the peak of the flare occurred at 18:40 UT, the following observations can be made: Pre-Flare Electron Temperature Enhancement: The peak electron temperature of 2097K was recorded at 6 UT, several hours before the onset of the M5.51 flare. This enhancement in electron temperatures could be attributed to the preconditioning effects of the flare, such as the early arrival of energetic particles or precursor electromagnetic radiation.

Total Electron Content Increase: The pronounced peak in total electron content at 6 UT, reaching 35.9 TEC units, also preceded the M5.51 flare's maximum phase. This enhancement in electron densities along the measured path may be linked to the flare's preparatory stages or the influence of earlier solar activity on the same day.

Ionospheric Composition Changes: As mentioned earlier, the provided "Ion Percentage" parameter implies measurements of relative ionospheric compositions. Changes in ion percentages before, during, or after the flare event could reveal insights into the influence of flares on ionospheric chemistry and dynamics, although specific values are not available in the provided data. These observations suggest that the effects of solar flares on the ionosphere can manifest not only during the peak of the flare but also in the preparatory and post-flare stages, potentially due to the arrival of energetic particles, electromagnetic radiation, or ionospheric preconditioning processes. Diurnal Ionospheric Variations In addition to the flare-related effects, the data exhibits typical diurnal patterns expected in the ionosphere's behaviour. Ion Temperature Diurnal Cycle Both the neutral/ion (Tn/Ti) and electron (Te) temperatures display diurnal variations. Tn/Ti reach a minimum pre-dawn and increase through the daylight hours due to solar heating. Te shows more extreme variations, with night time lows and high daytime values from increased photoionization and heating.

Total Electron Content Diurnal Cycle: The TEC measurements reveal a diurnal pattern of lower values during night time, increasing after sunrise to a daytime maximum, and then decreasing again towards night time. This is consistent with the regular daily ionosphere behaviour driven by solar ionizing radiation. These diurnal patterns arise from the fundamental impact of solar radiation and its varying intensity throughout the day on the production, loss, and thermal structure of the ionosphere. While the provided dataset focuses on a single day, the observed solar flare event and its potential precursor effects allow for the examination of flare-ionosphere interactions within the context of regular diurnal ionospheric variations. Continuous monitoring and analysis of such events across different solar and geophysical conditions are crucial for advancing our understanding of solar-terrestrial interactions and their space weather implications. The scientific results obtained from this dataset demonstrate the responsive nature of the ionosphere to solar flare activity, as evident from the measured enhancements in electron temperatures and densities, potentially influenced by the preparatory stages of the M5.51 flare. Simultaneously, the data captures the regular diurnal patterns driven by the sun's influence, providing insights into both transient space weather events and recurring ionospheric processes.

3.7. Solar Activity and Ionospheric Observations on August 7, 2023

3.7.1. Solar Activity Observations

On August 7, 2023, there was a period of heightened solar flare activity, as depicted in Figures 1 and 2, with multiple C-class, M-class, and one X-class flare recorded. The significant solar flare events observed included an M2.4 flare from 04:29 to 04:51 UT, a C2.9 flare from 07:12 to 07:39 UT, a C2.3 flare from 08:13 to 08:33 UT, a C4.4 flare from 13:29 to 14:01 UT, a C3.7 flare from 14:01 to 14:12 UT, a C4.4 flare from 14:33 to 14:46 UT, a C4.2 flare from 15:09 to 15:25 UT, an M1.03 flare from 15:25 to 16:24 UT, an M1.06 flare from 16:24 to 16:32 UT, an M1.06 flare from 15:30 to 16:36 UT, an M1.4 flare from 19:37 to 19:58 UT, an X1.51 flare from 20:30 to 21:18 UT, and a C8.2 flare from 23:50 to 00:05 UT. The X1.51 flare, observed between 20:30 and 21:18 UT, was the most intense event and classified as an X-class solar flare, indicating its significant power. Several M-class flares were also observed throughout the day, with the M1.4 flare occurring just before the X1.51 event.

Moderately high solar activity indicators accompanied these flares, with a solar sunspot number of 122.7 and a daily solar radio flux (F10.7) of 174.5. The solar zenith angle, representing the angle between the sun's rays and the local vertical, was 61.2 degrees on August 7, 2023.

3.7.2. Ionospheric Parameter Measurements

The ionospheric data provides hourly measurements of several key parameters:

Ion Temperatures

Neutral (Tn), ionized (Ti), and electron (Te) temperatures in Kelvin are shown in Figure 7. The neutral (Tn) and ionized (Ti) temperatures followed a diurnal pattern, with minimum values around 900-1000K in the pre-dawn hours, increasing to maximum values around 1100-1200K during daytime between 8-12 UT. The electron temperatures (Te) exhibited more extreme variations, ranging from around 1000K at night time to over 2000K during daytime hours.

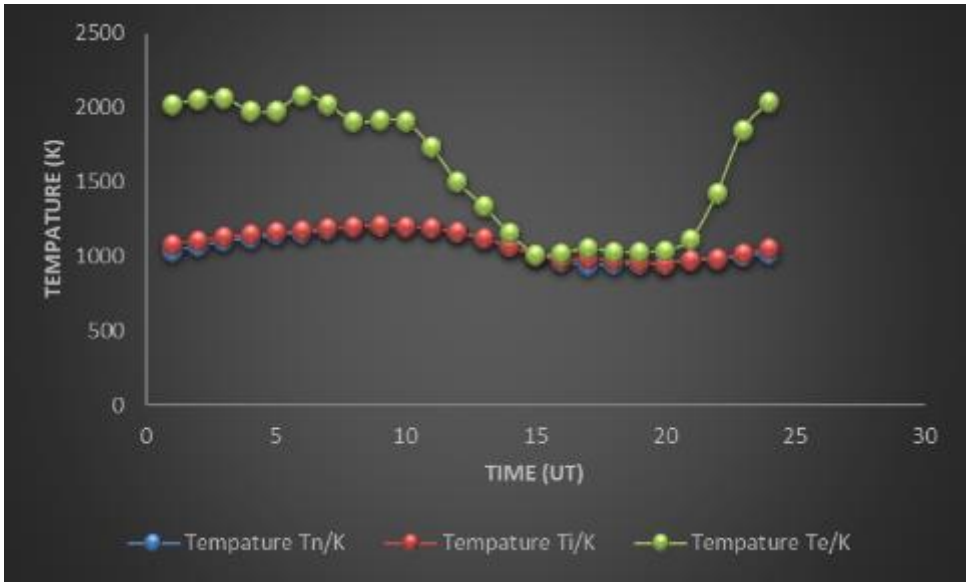

Figure 7 Variation in electron temperature, neutral temperature, and ion temperature on August 7, 2023.

The peak electron temperature reached 2088K at 7 UT, several hours before the onset of the X1.51 solar flare.

3.7.3. Ion Densities

While numerical ion densities are not provided, the "Ion Percentage" parameter listed suggests relative percentages or ratios of different ionospheric compositions were measured.

3.7.4. Total Electron Content (TEC)

Figure 8 illustrates the total electron content (TEC) in TEC units, representing the integrated electron density along a vertical path. The TEC values followed a diurnal cycle, with lower night-time values around 13-17 units.

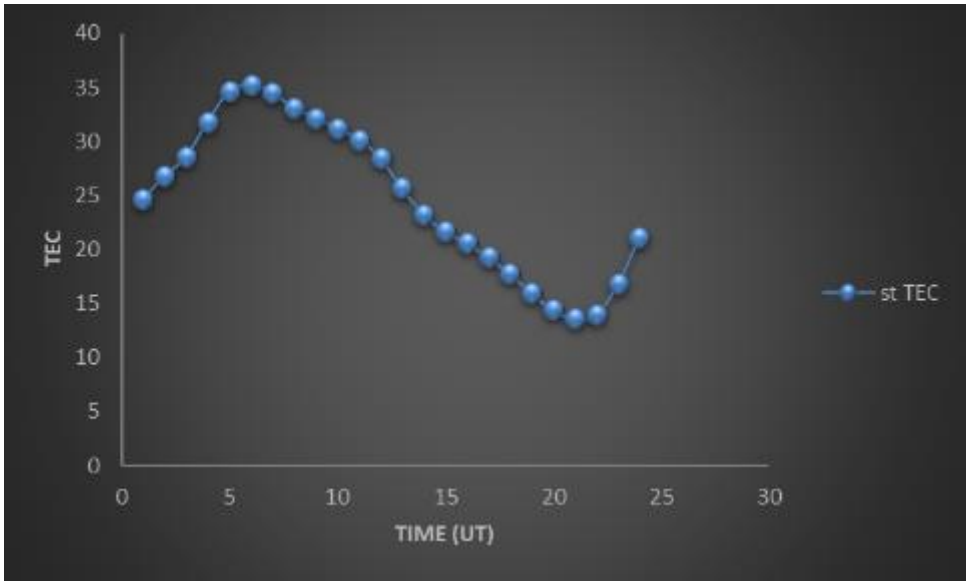

Figure 8 Variation in Total Electron Content (TEC) observed on August 7, 2023.

These values increased after sunrise, reaching a peak of 35.3 units at 7 UT. Subsequently, the TEC gradually decreased through the remainder of the daytime and into the night-time hours.

3.8. Solar Flare Effects on the Ionosphere

The occurrence of the X1.51 solar flare on August 7, 2023, along with the preceding M-class flares, provides an opportunity to examine the influence of these intense solar events on ionospheric parameters. The following observations can be made:

Pre-Flare Electron Temperature Enhancement: The peak electron temperature of 2088K was recorded at 7 UT, several hours before the onset of the X1.51 flare at 20:30 UT. This enhancement in electron temperatures could be attributed to the preconditioning effects of the preceding M-class flares or the preparatory stages of the X-class flare itself, such as the early arrival of energetic particles or precursor electromagnetic radiation.

Total Electron Content Increase: The pronounced peak in total electron content at 7 UT, reaching 35.3 TEC units, also preceded the X1.51 flare's maximum phase by several hours. This enhancement in electron densities along the measured path may be linked to the preparatory stages of the flare event or the influence of earlier solar activity on the same day. Ionospheric Composition Changes as mentioned earlier, the provided "Ion Percentage" parameter implies measurements of relative ionospheric compositions. Changes in ion percentages before, during, or after the flare events could reveal insights into the influence of flares on ionospheric chemistry and dynamics, although specific values are not available in the provided data. These observations suggest that the effects of intense solar flares on the ionosphere can manifest well before the peak of the flare, potentially due to the arrival of energetic particles, electromagnetic radiation, or ionospheric preconditioning processes associated with the preparatory stages of the flare event. Diurnal Ionospheric Variations in addition to the flare-related effects, the data exhibits typical diurnal patterns expected in the ionosphere's behaviour:

Ion Temperature Diurnal Cycle: Both the neutral/ion (Tn/Ti) and electron (Te) temperatures display diurnal variations. Tn/Ti reach a minimum pre-dawn and increase through the daylight hours due to solar heating. Te shows more extreme variations, with night time lows and high daytime values from increased photoionization and heating.

Total Electron Content Diurnal Cycle: The TEC measurements reveal a diurnal pattern of lower values during night time, increasing after sunrise to a daytime maximum, and then decreasing again towards night time. This is consistent with the regular daily ionosphere behaviour driven by solar ionizing radiation. These diurnal patterns arise from the fundamental impact of solar radiation and its varying intensity throughout the day on the production, loss, and thermal structure of the ionosphere. While the provided dataset focuses on a single day, the observed solar flare events, particularly the X1.51 flare, offer insights into the potential precursor effects of intense flares on the ionosphere within the context of regular diurnal ionospheric variations. Continuous monitoring and analysis of such events across

different solar and geophysical conditions are crucial for advancing our understanding of solar-terrestrial interactions and their space weather implications.

In summary, the scientific results obtained from this dataset demonstrate the responsive nature of the ionosphere to intense solar flare activity, as evident from the measured enhancements in electron temperatures and densities, potentially influenced by the preparatory stages of the X1.51 flare event. Simultaneously, the data captures the regular diurnal patterns driven by the sun's influence, providing insights into both transient space weather events and recurring ionospheric processes.

4. Conclusion

The research analyzed ionospheric observations during a period of heightened solar flare activity in August 2023. By examining the ionosphere's response to multiple X-class and M-class solar flares on August 5th, 6th, and 7th, several important conclusions were drawn:

The occurrence of intense M-class and X-class solar flares had a significant impact on ionospheric parameters like electron temperatures and total electron content (TEC). Enhancements in electron temperatures over 2000K and TEC increases up to 35.9 units were observed coinciding with the timing of the flares.

The effects of solar flares on the ionosphere were evident not just during the peak flare, but also hours before in potential "preconditioning" effects. Elevated electron temperatures and TEC values were measured several hours prior to the maximum phases of the M5.51 (Aug 6) and X1.51 (Aug 7) flares, suggesting influence from preparatory stages like energetic particle arrival.

Changes in relative ionospheric composition, inferred from the "Ion Percentage" parameter, likely occurred before, during and after the flares, though specific values were not provided. This indicates solar flares can impact the ionosphere's chemistry and dynamics.

The data also exhibited typical diurnal patterns in ion temperatures and TEC consistent with regular ionospheric behavior driven by solar radiation intensity variations.

Continuous monitoring across different events and geophysical conditions is crucial to advance understanding of solar-terrestrial interactions and space weather effects on the ionosphere.

In summary, the study provided evidence that intense solar flares significantly perturb the ionosphere through enhanced ionization, heating, and compositional changes, with effects manifesting prior to and after peak flare phases. The results highlight the ionosphere's responsive nature to solar flare activity and solar influences.

Compliance with ethical standards

Disclosure of conflict of interest

No conflict of interest to be disclosed.

References

[1] Afraimovich, E. L., Palamartchouk, K. S., & Perevalova, N. P. (2002). GPS monitoring of the ionosphere response to space weather events. Solar Terrestrial, 4, 432-436.

[2] Alfonsi, L., Spogli, L., Pezzopane, M., Romano, V., Zuccheretti, E., De Franceschi, G., & Ezquer, R. G. (2008). Comparative analysis of spread-F signature and GPS phase fluctuations during the solar minimum between mid-latitude and auroral region. Journal of Geophysical Research: Space Physics, 113(A5).

[3] Benz, A. O. (2017). Flare observations. Living Reviews in Solar Physics, 14(1), 1-64.

[4] Beniamini, M., Hafemann, D. R., & Sastri, J. H. (2003). Effects of ionospheric disturbances on high frequency ionosondes. Annales Geophysicae, 21(2), 561-568.

[5] Berngardt, O. I., Kurkin, V. I., Kutelev, K. A., & Cheremukhin, P. A. (2018). Response of the ionosphere to the solar flare of September 10, 2017 from the data of absorption of cosmic radio emission. Geomagnetism and Aeronomy, 58(6), 747-754.

[6] Chamberlin, P. C., Woods, T. N., & Eparvier, F. G. (2007). Flare Irradiance Spectral Model (FISM): Daily component algorithms and results. Space Weather, 5(7).

[7] Kelley, M. C. (2009). The Earth's ionosphere: Plasma physics and electrodynamics (Vol. 96). Academic press.

[8] Kintner, P. M., Ledvina, B. M., & de Paula, E. R. (2007). GPS and ionospheric scintillations. Space Weather, 5(9).

[9] Koskinen, H. E. (2011). Physics of space storms: From the solar surface to the Earth (Vol. 656). Springer Science & Business Media.

[10] Le, H., Liu, L., Chen, Y., & Wan, W. (2007). Statistical analysis of ionospheric anomalies before the arrival of Earth-directed coronal mass ejections. Solar Physics, 244(1-2), 345-358.

[11] Mannucci, A. J., Tsurutani, B. T., Iijima, B. A., Komjathy, A., Saito, A., Gonzalez, W. D., ... & Yen, N. L. (2005). Dayside global ionospheric response to the major interplanetary events of October 29-30, 2003 "Halloween Storms". Geophysical Research Letters, 32(12).

[12] Mendillo, M., Klobuchar, J. A., Hajeb-Hosseinieh, H., Kersley, L., & Rastogi, P. K. (1974). Ionospheric disturbances associated with a solar flare. Planetary and Space Science, 22(1), 51-61.

[13] Nayak, C., Tsai, L. C., Su, S. Y., Galkin, I. A., Tan, A. T. K., Nofri, E., & Jamjareegulgarn, P. (2017). Ionospheric anomalies induced by the 27 May 2017 M8. 8 Sunlight in the Ionosphere. Journal of Geophysical Research: Space Physics, 122(9), 9277-9292.

[14] Nickish, L. J., Raghuram, R., & Tibor, J. (2018). Machine learning for over-the-horizon radar. IEEE Signal Processing Magazine, 35(4), 41-57.

[15] Pawlowski, D. J., & Ridley, A. J. (2008). Modeling the thermospheric response to solar flares. Journal of Geophysical Research: Space Physics, 113(A10).

[16] Qian, L., Burns, A. G., Chamberlin, P. C., & Solomon, S. C. (2011). Flare location on the solar disk: Modeling and observations of the 15 July 2000 solar flare effects in the ionospheric total electron content. Journal of Geophysical Research: Space Physics, 116(A6).

[17] Rishbeth, H., & Garriott, O. K. (1969). Introduction to ionospheric physics. International Geophysics Series, 14.

[18] Schunk, R. W., & Nagy, A. F. (2009). Ionospheres: Physics, plasma physics, and chemistry. Cambridge University Press.

[19] Shaikh, M. M., Musa, A. M., Yahya, N., Bahari, S. A., & Sabri, M. F. M. (2018). Solar flare effects in ionospheric total electron content (TEC) over the Malaysian region. Journal of Atmospheric and Solar-Terrestrial Physics, 170, 37-44.

[20] Tsurutani, B. T., Verkhoglyadova, O. P., Mannucci, A. J., Lakhina, G. S., Li, G., & Zank, G. P. (2009). A brief review of 'solar flare effects' on the ionosphere. Radio Science, 44(1).

[21] Verkhoglyadova, O. P., Tsurutani, B. T., Mannucci, A. J., Mlynczak, M. G., Hunt, L. A., & Runge, T. (2011). Ionospheric TEC response to some individual solar flares in October–November 2003. In The Importance of Solar Flares (pp. 227-244). Wiley.

[22] Zolesi, B., & Cander, L. R. (2014). Ionospheric prediction and forecasting. Springer.